Communication

Wireless Electrochemical DNA Microarray Sensor

Kwok-Fan Chow, Franc#ois Mavre#, and Richard M. Crooks

More About This Article

Additional resources and features associated with this article are available within the HTML version:

- Supporting Information
- Links to the 1 articles that cite this article, as of the time of this article download
- Access to high resolution figures
- Links to articles and content related to this article
- Copyright permission to reproduce figures and/or text from this article

View the Full Text HTML

ACS Publications
High quality. High impact.

# Wireless Electrochemical DNA Microarray Sensor

Kwok-Fan Chow, François Mavré, and Richard M. Crooks*

Department of Chemistry and Biochemistry, Center for Electrochemistry, Texas Materials Institute, Center for Nano- and Molecular Science and Technology, The University of Texas at Austin, 1 University Station, A5300, Austin, Texas 78712-0165

Received March 18, 2008; E-mail: crooks@cm.utexas.edu

Here we report an electrochemical DNA microarray sensor whose function is controlled using just two wires regardless of the number of individual sensing electrodes. This advance is enabled by confining bipolar sensing electrodes within a microfluidic channel (part a of Scheme 1) and exerting potential control over the electrolyte solution rather than individual electrodes. In this configuration, the two driving electrodes control the potential difference between the sensing electrodes and the solution, and the current at the sensing electrodes is indirectly measured by taking advantage of electrogenerated chemiluminescence (ECL) present at the anode end of each bipolar electrode. In this communication, we show that this approach can be used to sense hybridization of DNA oligonucleotides.

Scheme 1
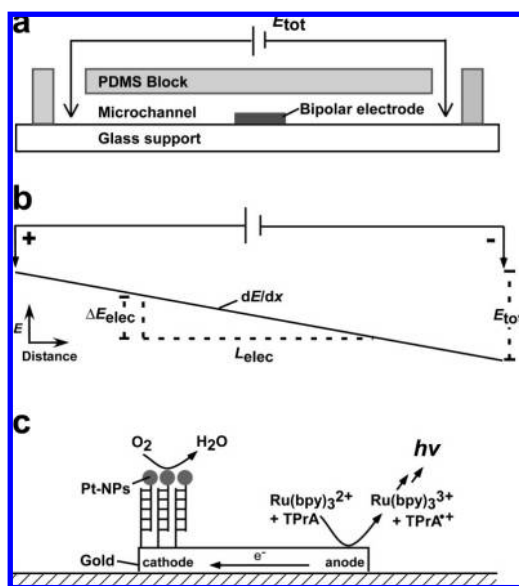
Electrochemistry is normally carried out by controlling the electrode potential. However, because the potential difference between the electrode and the solution drives the electron-transfer reaction, it is equally effective to control the potential of the solution. Our approach for using this principle is illustrated in part b of Scheme 1.[1,2] An external potential (E_{tot}) is applied to the two ends of a microchannel, and the resistance of the electrolyte solution results in a linear potential gradient (dE/dx) along the channel. The difference in potential between the two ends of the bipolar electrode (ΔE_{elec}) is the fraction of E_{tot} dropped across the length of this electrode (L_{elec}). If ΔE_{elec} is sufficiently large, then faradaic electrochemical processes will occur simultaneously at both ends of the bipolar electrode. Because of the requirement for charge balance, the rate of electron transfer (i.e., the current) at both ends of the electrode must be the same.
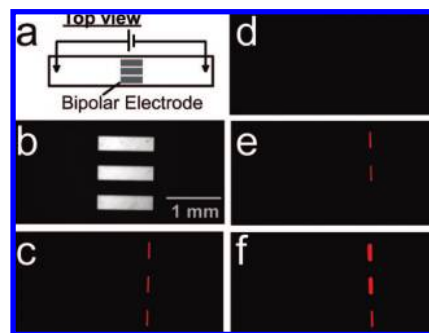

Figure 1. (a) Top-view schematic illustration of the microdevice. (b) Optical micrograph of the bipolar electrode configuration used to obtain the data in the other panels of this figure. False-color luminescence micrographs showing (c) the ECL emitted at $E_{tot} = 16.0$ V when complementary target DNA functionalized with Pt-NPs is hybridized to probe DNA present on the electrode surface; (d) no ECL emitted at 16.0 V prior to hybridization; (e) the ECL emitted at 16.0 V when only the top two electrodes of the device are exposed to the labeled target; and (f) the ECL emission at $E_{tot} = 22.0$ V for the device in (e).

A significant deficiency of bipolar electrochemistry is that there is no means for directly measuring current flowing within an electrode.[1,2] The experimental configuration illustrated in part c of Scheme 1 addresses this problem. Here, E_{tot} is held at a sufficiently high value that the ECL reaction resulting from the oxidation of Ru(bpy)$_3$$^{2+}$ and tri-n-propylamine (TPrA),[3–5] indicated at the anode end of the bipolar electrode, is activated upon electrocatalytic reduction of O$_2$ at the cathode end of the electrode. In the sensing experiments discussed next, the oxygen reduction reaction (ORR) is catalyzed by hybridization of target DNA labeled with Pt nanoparticles (Pt-NPs) to previously immobilized capture DNA.[6] Accordingly, in the presence of DNA hybridization at the cathode, light is emitted from the anode.

Part a of Figure 1 shows that the sensor consists of a microfluidic device and three Au electrodes. The poly(dimethylsiloxane) (PDMS) microfluidic device was prepared by a standard micromolding method.[7] The microchannel was 12 mm long, 1.75 mm wide, and 26 μm high. The three Au electrodes (1.00 × 0.25 mm) were microfabricated on a glass slide and configured parallel to one another at the center of the channel. Two Pt wires were placed in reservoirs at either end of the microfluidic channel and an external field was applied via a power supply.

Prior to assembly of the microfluidic device, the electrodes were modified with thiol-functionalized, 25-mer DNA capture probes (details regarding the DNA sequences, labeling procedures, and electrode modification are provided in the Supporting Information) by drop casting the DNA solution onto the electrodes and then back-filling vacancies within the resulting submonolayer with 6-mer-captohexanol. Next, the electrode array was exposed to a 0.1 μM solution of target DNA labeled with 4 nm Pt-NPs. Following this
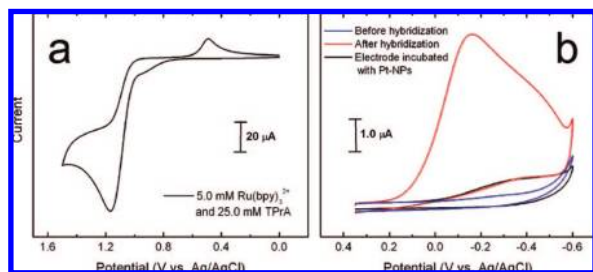
Figure 2. Cyclic voltammograms obtained from a macroscopic gold working electrode configured within a standard three-electrode cell. (a) The solution contained 5.0 mM Ru(bpy)$_3^{2+}$ and 25.0 mM TPrA in 0.100 M phosphate buffer. (b) The solution contained air-saturated 0.100 M phosphate buffer, and the CVs were obtained after modification of the electrode with probe DNA (blue), after hybridization with Pt-NP-labeled cDNA (red), and after incubation of a probe-modified electrode with a 100 nM solution of free Pt-NPs (no cDNA, black CV). Scan rate: 100 mV/s.

step and extensive rinsing, X-ray photoelectron spectroscopy confirmed the presence of Pt-NPs on the electrode surface (Figure S2, Supporting Information). Finally, the PDMS block containing the microchannel was mechanically attached to the glass slide, and the channel was filled with a solution consisting of 5.0 mM Ru(bpy)$_3^{2+}$ and 25.0 mM TPrA in 0.100 M phosphate buffer (pH 6.9).

Part b of Figure 1 is an optical micrograph of three bipolar electrodes present within the assembled microfluidic channel. Part c of Figure 1 is a luminescence micrograph of the same region of the fluidic channel shown in part b, but after application of a voltage of $E_{tot} = 16.0$ V. The red emission at the anode end of the bipolar electrodes results from ECL that is correlated to Pt-NP-catalyzed oxygen reduction at the cathode end. To ensure that the observed emission is related to the presence of the Pt-NP labels, the same experiment was performed, except without exposing the electrodes to the labeled DNA complement. In this case, no ECL is observed at $E_{tot} = 16.0$ V (part d), but at a higher voltage ($E_{tot} = 22.0$ V) ECL is observed due to an uncatalyzed faradaic process at the cathode end of the electrode. The important point is that the presence of labeled DNA is signaled by ECL at all three electrodes.

The observations presented thus far can best be understood in terms of cyclic voltammograms (CVs) obtained using a classical three-electrode cell and incorporating a macroscopic gold electrode modified using the same procedures used for the microcell. Part a of Figure 2 shows a CV obtained in this type of cell for a solution containing both Ru(bpy)$_3^{2+}$ and TPrA present at the same concentrations used to obtain the data in Figure 1. Both Ru(bpy)$_3^{2+}$ and TPrA undergo oxidation at about the same potential (∼1.1 V vs Ag/AgCl).[3–5] Part b of Figure 2 shows CVs corresponding to oxygen reduction. The red CV was obtained using a gold electrode modified with probe DNA hybridized to the complementary target labeled with Pt-NPs. A high current due to the Pt-catalyzed ORR is observed at about −0.1 V. Therefore, the voltage difference between the onset of Ru(bpy)$_3^{2+}$ and TPrA oxidation and oxygen reduction is ∼1.2 V. Using the assumptions embodied in part b of Scheme 1 and the numerical values used to obtain the data in part c of Figure 1 ($E_{tot} = 16.0$ V, channel length = 12 mm, $L_{elec} = 1.00$ mm), the calculated value of ΔE_{elec} is 1.3 V. That is, the potential difference (ΔE_{elec}) required for light emission (part c of Figure 1)

is nearly the same as the difference between the onset potentials for the ECL and ORR reactions shown in Figure 2. The blue CV in Figure 2 was obtained under the same conditions as the red CV, but in the absence of the Pt-NP-labeled DNA complement. In this case, the onset of the cathodic process is observed at a more negative potential, which is consistent with the observations discussed in relation to part d of Figure 1.

To demonstrate that the presence of Pt-NPs, and hence ECL emission, is directly correlated to DNA hybridization rather than to nonspecific adsorption (NSA), we prepared a macroscopic gold electrode, modified it with probe DNA, and then incubated it with a solution of Pt-NPs that were not conjugated to DNA. The resulting black CV (part b of Figure 2) indicates that the degree of oxygen reduction in this case is small compared to that resulting from hybridization of labeled DNA (red CV).

Parts e and f of Figure 1 indicate that the emission of ECL is not affected by neighboring electrodes. In this set of experiments, all three electrodes were modified with probe DNA, but only the top two were exposed to cDNA labeled with Pt-NPs. When $E_{tot} = 16.0$ V was applied across the fluidic channel, ECL was observed only at the two electrodes hybridized to the target. However, when E_{tot} was increased to 22.0 V, then the background cathodic process was initiated, resulting in light emission from all three electrodes. Consistent with the model shown in part b of Scheme 1, emission is more intense for the upper two electrodes at this higher voltage.

The important point of this paper is that the interfacial potential of multiple, well-defined bipolar electrodes can be controlled using just two wires. Moreover, the current flowing in these bipolar electrodes can be indirectly observed as light emission. Finally, chemical modification of the cathode ends of the bipolar electrodes with DNA results in a selective electrochemical array sensor. Forthcoming reports will quantavely address key issues such as accuracy, precision, selectivity, quantitation, and much larger numbers of bipolar electrodes.

Supporting Information Available: Information about the nanoparticle synthesis and their TEM characterization, electrode modification, and XPS analysis. This material is available free of charge via the Internet at http://pubs.acs.org.

References

(1) Zhan, W.; Alvarez, J.; Crooks, R. M. *J. Am. Chem. Soc.* **2002**, *124*, 13265–13270.
(2) Arora, A.; Eijkel, J. C. T.; Morf, W. E.; Manz, A. *Anal. Chem.* **2001**, *73*, 3282–3288.
(3) Leland, J. K.; Powell, M. J. *J. Electrochem. Soc.* **1990**, *137*, 3127–3131.
(4) Bard, A. J. *Electrogenerated Chemiluminescence*; Marcel Dekker: New York, 2004.
(5) Miao, W.; Choi, J.-P.; Bard, A. J. *J. Am. Chem. Soc.* **2002**, *124*, 14478–14485.
(6) Polsky, R.; Gill, R.; Kaganovsky, L.; Willner, I. *Anal. Chem.* **2006**, *78*, 2268–2271.
(7) Xia, Y.; Whitesides, G. M. *Angew. Chem., Int. Ed.* **1998**, *37*, 550–575.

JA802013Q